Heliyon 10 (2024) e37898

Contents lists available at ScienceDirect

Heliyon

journal homepage: www.cell.com/heliyon

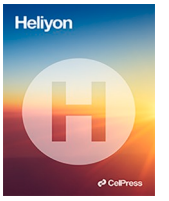

Research article

The influence of spatial distribution and transcriptional regulation of secondary metabolites on the bioactivities of *Adenophora triphylla* (Japanese lady bell)

Seon Young Yoon [a], Seon-Woong Kim [b], Tae Kyung Hyun [a,*]

[a] *Department of Industrial Plant Science and Technology, College of Agriculture, Life and Environment Sciences, Chungbuk National University, Cheongju, 28644, Republic of Korea*
[b] *Department of Agricultural Economics, College of Agriculture, Life and Environment Sciences, Chungbuk National University, Cheongju, 28644, Republic of Korea*

ARTICLE INFO

Keywords:
Adenophora triphylla
Phenylpropanoid
Secondary metabolite
Transcriptome
YABBY transcription factor

ABSTRACT

The distribution of secondary metabolites in plant tissues plays a crucial role in determining their pharmacological properties. In this study, we investigated the dynamics of the bioactive compounds in *Adenophora triphylla*, a medicinal herb with diverse therapeutic applications.

The anti-inflammatory properties of the EtOAc fraction from the aerial part extract (A_ EtF) exhibited an IC_{50} value of 27.2 ± 2.3 μg/mL, significantly surpassing that of the EtOAc fraction from the root extract (R_EtF) with an IC_{50} of 38.9 ± 2.9 μg/mL. Similarly, the anti-melanogenic activity of A_EtF (IC_{50} = 68.9 ± 2.3 μg/mL) outperformed that of R_EtF (IC_{50} = 90.0 ± 5.5 μg/mL). Analysis of the distinct chemical profiles of these tissues using UPLC-ESI-Q-TOF-MS revealed that the distribution of secondary metabolites contributes to the observed variations in pharmacological properties between the aerial parts and roots. Transcriptome analysis further elucidated spatially regulated genes associated with secondary metabolism, highlighting the role of AbtYABBYs as potential regulators of phenylpropanoid biosynthesis. To validate their function, these genes were transiently expressed in tobacco leaves via agro-infiltration, confirming their role in modulating polyphenolic compound biosynthesis. Our findings underscore the importance of understanding spatial gene expression patterns for harnessing the complete pharmacological potential of medicinal plants. This study provides valuable insights into the spatial regulation of secondary metabolism and lays the groundwork for targeted manipulation of plant bioactivity for therapeutic and industrial applications.

1. Introduction

Plants synthesize a diverse array of secondary metabolites that are not only a key part of the defense mechanism against pathogenic attacks and environmental stresses but also an important sources of new lead compounds in drug discovery research [1]. In general, the precursors of secondary metabolites are derived from relatively few primary metabolic pathways, including photosynthesis, glycolysis, and the tricarboxylic acid cycle [2]. In *Panax japonicus*, the upstream parts of triterpenoid saponin biosynthesis occur in leaves, whereas UDP-glycosyltransferases exhibit higher expression in roots compared to leaves [3]. This indicates that photosynthetic organs

* Corresponding author.
E-mail address: taekyung7708@chungbuk.ac.kr (T.K. Hyun).

https://doi.org/10.1016/j.heliyon.2024.e37898
Received 3 April 2024; Received in revised form 29 August 2024; Accepted 12 September 2024
Available online 13 September 2024

are the primary sites for secondary metabolite biosynthesis, while storage organs serve as sites for their modification. However, nicotine is synthesized in tobacco roots and accumulates in the leaf vacuoles [4]. This suggests that the spatial accumulation of specific secondary metabolites is strongly dependent on the transcription of biosynthetic genes and transport systems [5,6]. Such spatial patterns can cause variations in the pharmacological properties of different plant organs.

Since ancient times, medicinal or folk plants have been integral to traditional medicine for primary health care. Today, these plants are increasingly being utilized as dietary supplements for disease prevention and as alternative or complementary medicine [7,8]. Information from ancient oriental medicine plays an essential role in the development of new products using medicinal plants. Artemisinin from *Artemisia annua* is an important example of how ancient recipes and records are applied in a holistic approach in present-day health care [9]. However, while ancient recipes and records offer natural avenues to discover treatments for health issues, they may also introduce biases against certain materials. For example, the root is the most commonly used part of *Panax ginseng* in oriental medicine, making it the most-consumed dietary supplement worldwide [10]. In contrast, other parts of ginseng, such as leaves, flowers, and fruits were historically considered useless by-products [11,12]. However, current pharmaceutical studies and phytochemical analyses have revealed the potential of ginseng by-products as beneficial biomaterials for the food, cosmetic and medical industries [11–16]. These findings indicate that systematic investigations, including analyses of spatial patterns and pharmacological properties of phytochemicals, are necessary for the development of potential main sources of medicinal compounds.

Adenophora triphylla var. japonica, commonly known as Japanese lady bell, is a perennial herbaceous plant belonging to the Campanulaceae family. Its root has been traditionally used in oriental medicine to treat patients with lung diseases, such as cough, sputum, asthma and airway inflammatory diseases [17], whereas young aerial parts or sprouts of *A. triphylla* have been utilized as food ingredients [18]. As evidence for this, the root extracts of *A. triphylla* exhibit anti-inflammatory, anti-obesity and anti-cancer activities [19–23]. Contrastively, young aerial parts have been utilized only as vegetables [18], although the presence of bioactive phenolic compounds like chlorogenic acid in the aerial parts of *A. triphylla* suggests their potential as dietary health supplements [24]. However, information regarding the chemical composition and biochemical activities of the aerial parts of *A. triphylla* is currently insufficient.

To address this research gap, we conducted a comparative analysis of the bioactivities of *A. triphylla* aerial part and root extracts. UPLC-Q-TOF-MS and transcriptome analyses were employed to understand the difference in bioactivities between aerial parts and roots. Furthermore, *A. triphylla* YABBYs (AdtYABBYs) were identified to regulate the spatial expression patterns of flavonoid biosynthetic genes.

2. Materials and methods

2.1. Plant materials and extract preparation

Plant materials, specifically aerial parts and roots of two-month-old *A. triphylla* plants, were obtained from the Chungcheongbuk-do Agricultural Research & Extension Service, Repabulic of Korea in May 2022. These materials were freeze-dried and used for preparing 70 percent ethanol extracts. After evaporation, the dried powder extracts were suspended in water, and four solvent fractions were obtained using the fractional solvent extraction method described by Kim and Hyun [25]. Each solvent fraction was evaporated using a rotary evaporator for further analysis. Then, the samples were sterilized through filtration using a 0.2 μM sterile syringe filter membrane.

2.2. Determination of nitric oxide (NO) production

To determine NO production, RAW 264.7 macrophage cells (KCLB No. 40071, Korea Cell Line Bank, Seoul, Korea) were incubated with different concentrations of each extracts in the presence of 1 μg/mL lipopolysaccharide (LPS). Following a 24-h incubation at 37 °C, NO production was assessed using a Griess reagent kit (Promega, Madison, WI, USA), following the manufacturer's protocol.

2.3. Determination of anti-melanogenic properties

Mouse melanoma cell (B16F10 cell line, KCLB No. 80008, Korea Cell Line Bank, Seoul, Korea) stimulated with 3-isobutyl-1-methylxanthine (IBMX) were exposed to varying concentrations of the samples. Following a 48-h incubation in a CO_2 incubator, IBMX-induced melanin content was quantified following the method outlined by Ahn et al. [26]. B16F10 melanoma cells were treated with each extract and 100 μM IBMX and incubated at 37 °C for 48 h. After incubation, the cells were washed twice with ice-cold PBS and harvested by centrifugation. The pellets were solubilized in 1 N NaOH with 10 percent dimethyl sulfoxide at 65 °C for 1 h. The amount of melanin was determined by a microplate reader at 490 nm.

Tyrosinase inhibition was assessed using a tyrosinase inhibitor screening kit (BioVision, Milpitas, CA, USA), following the manufacturer's instructions, with kojic acid as a positive control.

2.4. Cytotoxicity analysis

The cytotoxicity of the samples against RAW264.7 and B16F10 cells was assessed using a tetrazolium-based colorimetric MTT assay, following the protocol outlined by Bang et al. [27]. The resulting formazan crystals were dissolved in DMSO, and their absorbance was measured at 550 nm to assess cell viability.

2.5. Determination of gene expression

Total RNA was isolated from RAW 264.7 and B16F10 cells using the TRIzol reagent. Subsequently, cDNA was synthesized, and the transcription levels of each gene were analyzed using quantitative real-time PCR (qRT-PCR) as described by Bang et al. [27]. β-actin was used for the normalization of each expression level, and the specific primer pairs used for qRT-PCR are listed in Supplemental Table 1.

2.6. Phytochemical analysis

Total phenolic (TPC) and total flavonoid (TFC) contents in the EtOAc fractions of both extracts were determined as described by Jin et al. [15].

A UPLC-Q-TOF-MS system equipped with a C18 column (2.1 mm × 100 mm, particle size 1.7 μm) was employed to analyze the metabolites in both EtOAc fractions, as described by Shin et al. [28]. The mass spectrometric analysis was performed under optimized conditions. The capillary voltage and cone voltage were set at 2.5 kV and 20 V, respectively. The nebulized gas flow rate was maintained at 900 L/h with a temperature of 100 °C in positive/negative mode, while the cone gas flow rate was set at 30 L/h. The mass range scanned ranged from 50 to 1500 *m/z*. The selected peaks were identified using the ChemSpider database in the UNIFI and METLIN datasets [28].

2.7. De novo transcriptome analysis

The total RNA from both aerial parts and roots was pooled in equivalent quantities and a cDNA library was prepared following the method outlined by Choi et al. [29]. The Illumina HiSeq 2500 sequencing platform was used for paired-end sequencing. After cleaning the raw sequencing reads, de novo assembly was performed using the Trinity platform [30]. The unigenes were identified through sequence similarity comparison against various databases, including the Kyoto Encyclopedia of Genes and Genomes (KEGG) pathway, Blast2GO and Non-Redundant (NR) databases. All raw reads were deposited in the NABIC database (National Agricultural Biotechnology Information Center; aerial parts, NN-8847; roots, NN-8848).

The expression levels of each unigene were analyzed using fragments per kilobase of transcript per million reads mapped (FPKM)

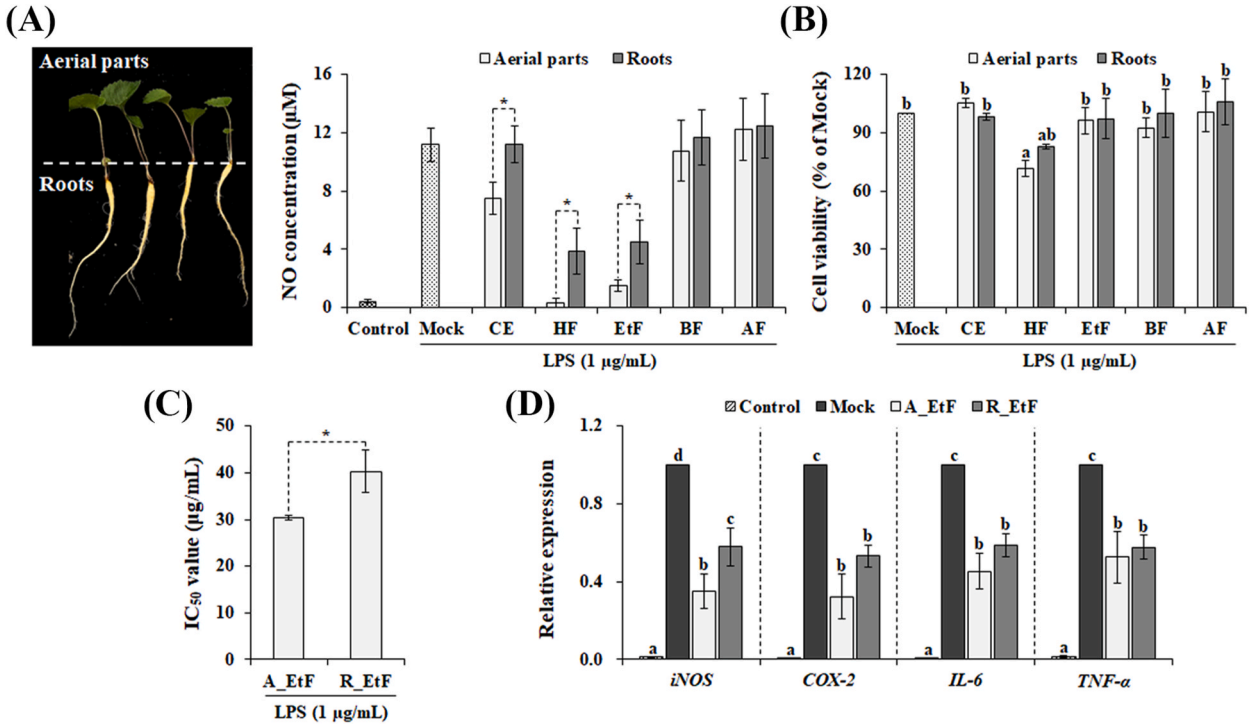

Fig. 1. Anti-inflammatory effects of the *Adenophora triphylla* aerial part extract and root extract on LPS-stimulated RAW264.7 macrophages. (A) Inhibition of NO production and (B) cytotoxicity of crude extracts (100 μg/ml) and their solvent fractions (50 μg/ml) in LPS-treated RAW264.7 cells. (C) IC_{50} values for the inhibition of LPS-induced NO production by A_EtF and R_EtF. (D) Impact of A_EtF and R_EtF on LPS-induced pro-inflammatory gene expression.Data represent the mean (±SE) of three independent experiments, with asterisks (*$p < 0.05$, *t*-test) or distinct letters ($p < 0.05$, Duncan's multiple range test). Mock, DMSO treatment; CE, crude extract; HF, hexane fraction; EtF, EtOAc fraction; BF, BuOH fraction; AF, aqueous fraction; A_EtF, EtOAc fraction of aerial part extract; R_EtF, EtOAc fraction of root extract.

method and differentially expressed genes (DEGs) were determined based on a *p*-value cutoff of 0.05 and |log2 (fold change)| ≥ 1.

2.8. Transient expression of AdtYABBY1 and AdtYABBY2 in tobacco

The complete *AdtYABBY1* (NABIC, NS-3500) and *AdtYABBY2* (NABIC, NS-3501) sequences were individually inserted into the pGWB505 binary vector and subsequently introduced into *Agrobacterium tumefaciens* strain GV3101. For transient expression in tobacco (*Nicotiana benthamiana*), agro-infiltration was conducted following the method outlined by Kim and Hyun [31]. Leaf TFC content and the expression levels of flavonoid biosynthetic genes were evaluated 4 d post-infiltration. The transient expression analysis was conducted in triplicate.

2.9. Statistical analysis

The experimental results are presented as the mean ± standard error (SE) of three independent experiments. Student's t-test ($p < 0.05$) was employed for comparing between two groups and Duncan's multiple range test ($p < 0.05$) was utilized to ascertain significance across multiple groups.

3. Results and discussion

3.1. Comparative evaluation of anti-inflammatory properties

Inflammation model via stimulating macrophage RAW264.7 cells with LPS is predominantly used as a model for characterizing the anti-inflammatory activity of various natural compounds [32]. To compare the anti-inflammatory activities of *A. triphylla* extracts, the inhibitory effect of each sample on the production of the pro-inflammatory mediator NO in LPS-treated RAW264.7 cells was evaluated. As shown in Fig. 1A, LPS treatment resulted in a 23-fold induction of NO production compared to non-treated cells (control), whereas treatment with the aerial part extract at a concentration of 100 μg/mL inhibited LPS-induced NO production by over 38.4 percent beyond the level observed in the mock group. Although the crude root extract did not exhibit appreciable activity, solvent fractionation led to an increase in its anti-inflammatory activity. Among the various solvent-partitioned fractions of both extracts, the hexane fractions (HFs) exhibited the highest anti-inflammatory activity, followed by the EtOAc fractions (EtFs). However, HFs (50 μg/mL)

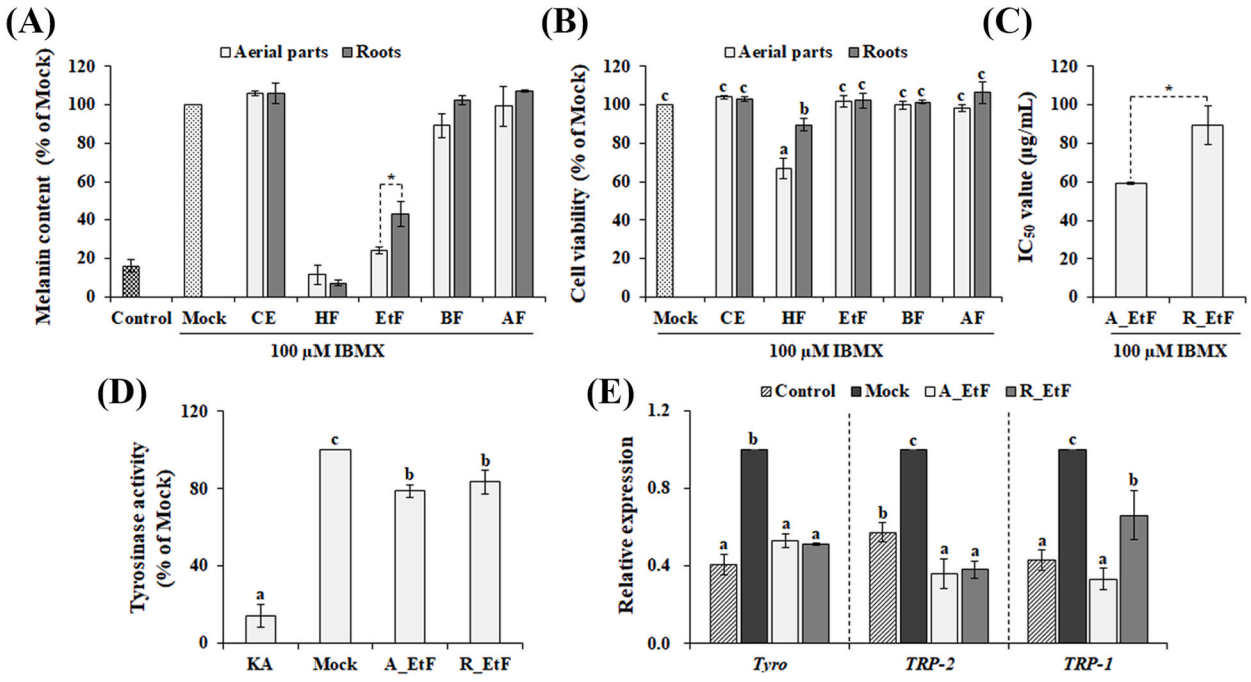

Fig. 2. Anti-melanogenic effects of *Adenophora triphylla* aerial part extract and root extract on IBMX-stimulated B16F10 cells. (A) Inhibition of melanin productionand (B) cytotoxicity (B) of crude extracts (200 μg/ml) and their solvent fractions (100 μg/ml) in IBMX-stimulated B16F10 cells. (C) IC_{50} values for melanin production induced by IBMX in the EtOAc fractions. (D) Inhibitory effect of A_EtF and R_EtF on cell-free tyrosinase activity. (E) Influence of A_EtF and R_EtF on the transcription of melanogenesis-related genes in IBMX-treated B16F10 cells. Data are presented as mean ± SE of three independent experiments. Statistical significance: $p < 0.05$ (*t*-test), distinct letters ($p < 0.05$, Duncan's test). Mock, DMSO treatment; CE, crude extract; HF, hexane fraction; EtF, EtOAc fraction; BF, BuOH fraction; AF, aqueous fraction; A_EtF, EtOAc fraction of aerial part extract; R_EtF, EtOAc fraction of root extract; Tyro, tyrosinase; TRP-1, tyrosinase-related protein 1; TRP-2, tyrosinase-related protein 2.

significantly suppressed the LPS-induced proliferation of RAW 264.7 cells, whereas EtFs (50 μg/mL) demonstrated no cytotoxic effects (Fig. 1B). Similar to our findings, the HF of the 80 percent ethanol root extract exhibited cytotoxicity against RAW 264.7 cells [17]. This suggests that the inhibition of LPS-induced NO production by HFs is associated with their cytotoxic effects. The anti-inflammatory properties of the EtF of the aerial part extract (A_EtF; $IC_{50} = 27.2 \pm 2.3$ μg/mL) were significantly superior to those of the EtF of the root extract (R_EtF; $IC_{50} = 38.9 \pm 2.9$ μg/mL), highlighting the stronger anti-inflammatory properties of aerial parts compared to roots (Fig. 1C). Additionally, LPS-induced transcription levels of pro-inflammatory mediators and cytokines, including nitric oxide synthase (*iNOS*), cyclooxygenase-2 (*COX-2*), interleukin-6 (*IL-6*) and tumor necrosis factor-α (*TNF-α*), were significantly suppressed by both EtFs (Fig. 1D). This suggests that despite differences in activity levels, both root and aerial part extracts exhibit anti-inflammatory activity through the same mechanism.

3.2. Comparative evaluation of anti-melanogenic properties

As naturally derived bioactive compounds and extracts continue to undergo screening for the development of anti-melanogenic agents, the extract of *A. triphylla* has emerged as a promising candidate for addressing conditions associated with melanin hyperpigmentation [33]. However, this discovery was made through cell-free tyrosinase inhibition assay. Therefore, the anti-melanogenic properties of *A. triphylla* extracts were investigated using B16F10 murine melanoma cells. As depicted in Fig. 2A, treatment with 200 μg/mL of aerial part and root extracts inhibited IBMX-induced melanin accumulation by 63.2 percent and 5.7 percent, respectively. Among the solvent-partitioned fractions of both extracts, the HFs (100 μg/mL) exhibited the highest anti-melanogenic properties,

Table 1
Phytochemical constituents in the EtOAc fractions of *Adenophora triphylla* aerial part extract (A_EtF) and root extract (R_EtF).

Mode	Peak No.	Neutral Mass (Da)	Observed *m/z*	Formula	Proposed Molecule	Fragment Ions	Peak area
Positive	1	146.03678	146.036	$C_9H_6O_2$	Isocoumarin	91, 119	A_EtF > R_EtF
	2	610.15338	610.1533	$C_{27}H_{30}O_{16}$	Rutin	153, 303, 465	A_EtF > R_EtF
	3	550.09587	550.0966	$C_{24}H_{22}O_{15}$	Quercetin 3-O-malonylglucoside	109, 159, 303, 345	A_EtF > R_EtF
	4	608.17412	608.1746	$C_{28}H_{32}O_{15}$	Diosmin	147, 286, 301, 463	A_EtF > R_EtF
	5	564.11152	564.1121	$C_{25}H_{24}O_{15}$	Isorhamnetin 3-(6″-malonylglucoside)	127, 286, 301, 317, 463	A_EtF > R_EtF
	6	578.12717	578.1281	$C_{26}H_{26}O_{15}$	Tricin 7-(6-malonylglucoside)	301, 463	A_EtF > R_EtF
	7	519.33249	519.334	$C_{26}H_{52}NO_6P$	LPC(18:2)	104, 184, 258, 443, 502	A_EtF < R_EtF
	8	495.33249	495.3338	$C_{24}H_{50}NO_7P$	LPC(16:0)	104, 124, 258, 419, 478	A_EtF < R_EtF
	9	521.34814	521.3495	$C_{26}H_{52}NO_7P$	LPC(18:1)	104, 184, 258, 339, 504	A_EtF < R_EtF
	10	606.24783	606.2479	$C_{35}H_{34}N_4O_6$	Pheophorbide b	519, 547, 579	A_EtF > R_EtF
	11	592.26857	592.2689	$C_{35}H_{36}N_4O_5$	Pheophorbide a	461, 533, 561, 575	A_EtF > R_EtF
Negative	12	354.09508	354.0947	$C_{16}H_{18}O$	(neo, crypto)Chlorogenic acid	135, 179, 191	A_EtF > R_EtF
	13	338.10017	338.0998	$C_{16}H_{18}O_8$	p-Coumaroylquinic acid	119, 191, 215	A_EtF > R_EtF
	14	368.11	367.1028	$C_{17}H_{20}O_9$	Feruloylquinic acid	134, 149, 193	A_EtF > R_EtF
	15	1174.2972	1219.2954	$C_{53}H_{59}O_{30+}$	Violdelphin	93, 191, 449, 609	A_EtF > R_EtF
	16	464.0946	463.0873	$C_{21}H_{20}O_{12}$	Isoquercetin	243, 301	A_EtF > R_EtF
	17	478.0737	477.0664	$C_{21}H_{18}O_{13}$	Miquelianin	301, 461, 463	A_EtF > R_EtF
	18	506.10604	506.1053	$C_{23}H_{22}O_{13}$	6″-O-Acetylisoquercitrin	300	A_EtF > R_EtF
	19	564.1472	563.1399	$C_{26}H_{28}O_{14}$	Apiin	191, 337, 489	A_EtF > R_EtF
	20	208.0738	207.0665	$C_{11}H_{12}O_4$	Dimethoxycinnamic acid	133, 135, 161, 179	A_EtF > R_EtF
	21	504.3437	503.3364	$C_{30}H_{48}O_6$	Madecassic acid	503	A_EtF > R_EtF
	22	676.36701	676.367	$C_{33}H_{56}O_{14}$	Gingerglycolipid A	277, 397, 415	A_EtF > R_EtF

followed by the EtFs. However, the inhibition of B16F10 cell proliferation by HFs was comparable to that observed in RAW264.7 cells (Fig. 2B), indicating that the inhibitory effects of HFs on melanin accumulation are attributed to cytotoxicity. Additionally, the anti-melanogenic properties of A_EtF (IC_{50} = 68.9 ± 2.3 μg/mL) were significantly greater than that of R_EtF (IC_{50} = 90.0 ± 5.5 μg/mL) (Fig. 2C). Previous reports have indicated that the anti-melanogenic properties of *A. triphylla* roots and leaves are mediated by inhibiting the activity of tyrosinase [33], which is consistent with our findings (Fig. 2D). Furthermore, we found that treatment with A_EtF and R_EtF also resulted in the suppression of the IBMX-induced transcription of tyrosinase (*Tyro*) and tyrosinase-related protein-1 and -2 (*TRP-1* and *TRP-2*) (Fig. 2E), suggesting that both samples displayed anti-melanogenic activity via a common mechanism, regardless of the differences in their respective activity levels.

3.3. Distribution of metabolites between aerial parts and roots

As described above, the tissue-specific distribution of metabolites contributes to the variation in pharmacological properties between aerial parts and roots. To characterize the spatial distribution of metabolites between aerial parts and roots, untargeted qualitative analysis of EtOAc fractions was performed using UPLC-ESI-Q-TOF-MS (Supplementary Fig. 1), a method widely recognized for its exceptional mass measurement accuracy, superior separation resolution and remarkable sensitivity in comprehensive analysis of multiple components in plant extracts [34]. As presented in Table 1, a total of 22 compounds, including isocoumarin (1) and rutin (2), were identified in both A_EtF and R_EtF. R_EtF contained higher amounts of lysophosphatidylcholines (LPCs; 16:0, 18:1, 18:2), which are bioactive phospholipids known to function as lipid mediators in cellular responses and pathophysiology [35]. In tobacco, LPC levels increased during pathogen infection, with LPC 18:1 serving as a signaling molecule during pathogen-induced response [35]. This suggests that the higher amount of LPS in R_EtF may be attributed to the presence of soil microorganisms. A_EtF contained higher amounts of 19 compounds, including isocoumarin (1), rutin (2) and diosmin (4), which are known for their diverse pharmacological properties, such as anticancer, anti-inflammatory and antiviral activities [36–38]. Furthermore, the presence of pheophorbides (10 and 11), chlorophyll metabolites produced during senescence and/or fruit ripening [39], in A_EtF suggests their promising potential as bioactive compounds for treating cancer, viral infections and inflammatory disorders [40,41]. While further investigation is required to determine the synergistic and antagonistic effects of compound mixtures, the observed variations in pharmacological properties between the aerial parts and roots are likely attributed to the spatial distribution of these metabolites.

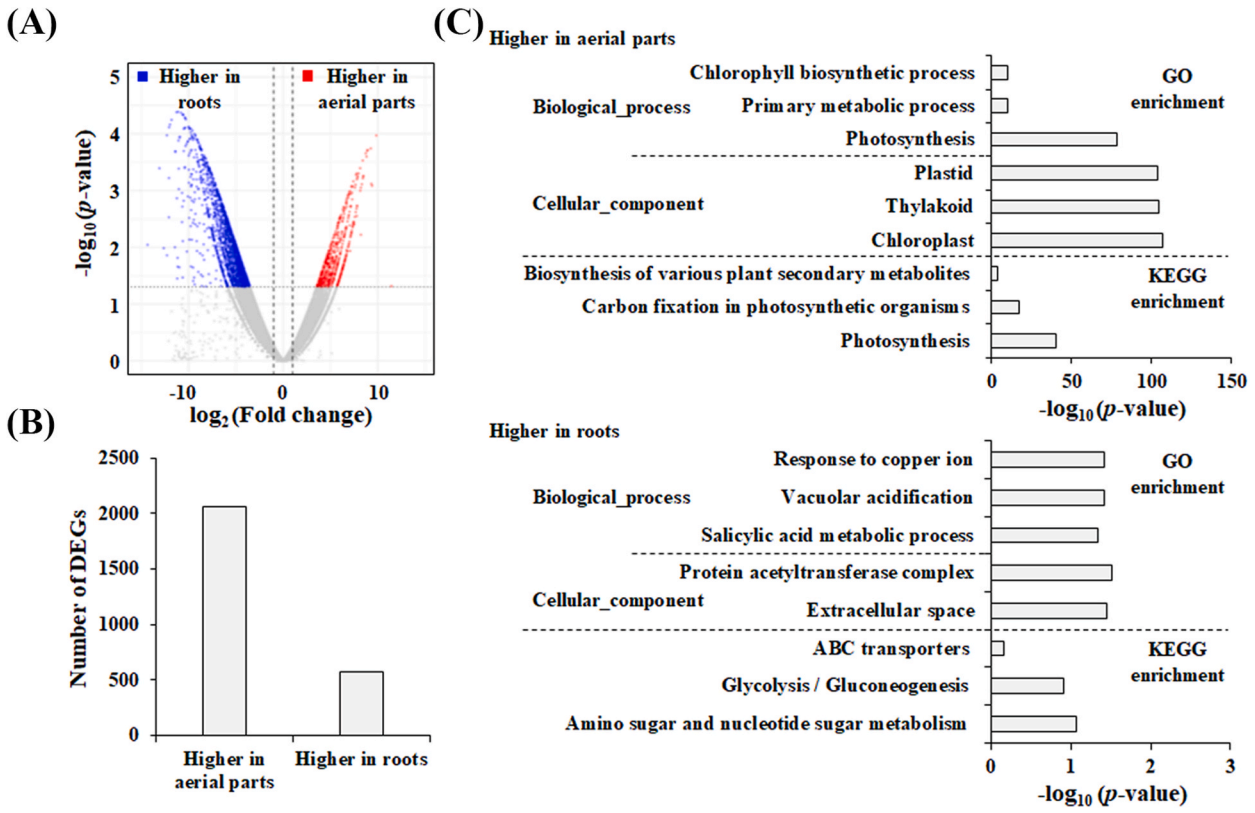

Fig. 3. Differential gene expression between the aerial parts and roots of *Adenophora triphylla*. (A) Volcano plot analysis and (B) the number of the differentially expressed genes (DEGs) (aerial parts vs. roots). (C) GO and KEGG enrichment analyses of the DEGs.

3.4. Variations in the transcription of functional genes

The accumulation of secondary metabolites is primarily influenced by the transcription of key genes involved in biosynthetic pathways [5], highlighting the necessity of analyzing transcriptional networks to comprehend the spatial distribution of metabolites. To analyze expression patterns, a cDNA library was generated using the Illumina 2500 platform. Subsequently, high-quality reads were de novo assembled using the Trinity program, resulting in 95,397 contigs with an average length of 1212 bp, with half of the contigs exceeding 1.6 kb in length (N50 = 1655 bp) (Supplementary Table 2). To explore the potential functions of the assembled unigenes, a similarity search was conducted against genome databases (Supplementary Table 2). A total of 68,569 unigenes (71.88 % of all unigenes) exhibited significant similarity to known proteins in the NR database (Supplemental Table 3). Subsequently, DEGs between aerial parts and roots were identified using a specified cutoff, as illustrated on a Volcano plot (Fig. 3A). A total 2626 of DEGs were identified, with 2058 genes highly expressed in aerial parts and 568 genes highly expressed in roots (Fig. 3A). The Gene Ontology (GO) analysis of highly expressed genes in aerial parts revealed their involvement in chlorophyll biosynthetic processes, primary metabolic processes, and photosynthesis. In contrast, the root-expressed genes were identified to be involved in vacuolar acidification, salicylic acid metabolic processes and response to copper ions (Fig. 3B). Vacuolar acidification and salicylic acid metabolic processes are essential for plant immunity [42,43]. Additionally, copper ion is known to activate plant immunity by suppressing ABA synthesis [44]. Thus, the GO analysis clearly demonstrated the functional roles of the aerial parts as source organs and the roots as defense barriers against pathogens.

The MapMan analysis revealed that the highly expressed genes in aerial parts were distributed across various secondary metabolic pathways, including those associated with flavonoids, lignin and phenols (Fig. 4A). Additionally, the TFC and TPC of aerial parts were higher than those of roots (Fig. 4B and C), indicating that the remarkably different accumulation of polyphenolic compounds between aerial parts and roots resulted from distinct gene expression patterns. Consistent with these findings, previous studies have reported that the expression patterns of genes involved in phenylpropanoid biosynthetic pathways positively influence the spatial distribution of polyphenolic compounds in various plants [45–47]. In higher plants, polyphenolic compounds are biosynthesized in a light-dependent manner and serve to protect the photosynthetic apparatus against photoinhibition caused by excessive light exposure [48–50]. Therefore, the higher efficiency of polyphenolic compound biosynthesis in aerial parts compared to roots may be attributed to light-induced activation of biosynthetic pathways, resulting in variations in pharmacological properties between these organs.

3.5. Variations in phenylpropanoid biosynthesis by AbtYABBYs

Various transcription factors (TFs), including MYB, basic helix-loop-helix, basic leucine zipper, WD40 and zinc finger proteins, either positively or negatively regulate phenylpropanoid biosynthesis [51]. Among these TFs, YABBY, a unique TF in seed plants, has received considerable attention as a positive regulator of phenylpropanoid biosynthesis [52–54]. For example, Arabidopsis YABBY1 (FILAMENTOUS FLOWER/YAB1) activates a subset of jasmonate-regulated genes, resulting in the accumulation of anthocyanin [52]. In *A. annua*, the overexpression of AaYABBY5 significantly induces the transcription of genes involved in the flavonoid biosynthetic pathway [53]. Based on these findings, it is hypothesized that spatial variations in polyphenolic compounds are mediated by the differential expression of AbtYABBYs. To test this hypothesis, it was first identified unigenes encoding six putative enzymes in our *A. triphylla* transcriptome library. Then, it was identified two AbtYABBYs that exhibited a higher expression in aerial parts compared to roots (Supplementary Fig. 2). To confirm that the two putative AbtYABBYs belong to the YABBY family, the presence of the zinc finger-like domain and the YABBY domain, conserved structural motifs characteristic of the YABBY family [54], was analyzed. As

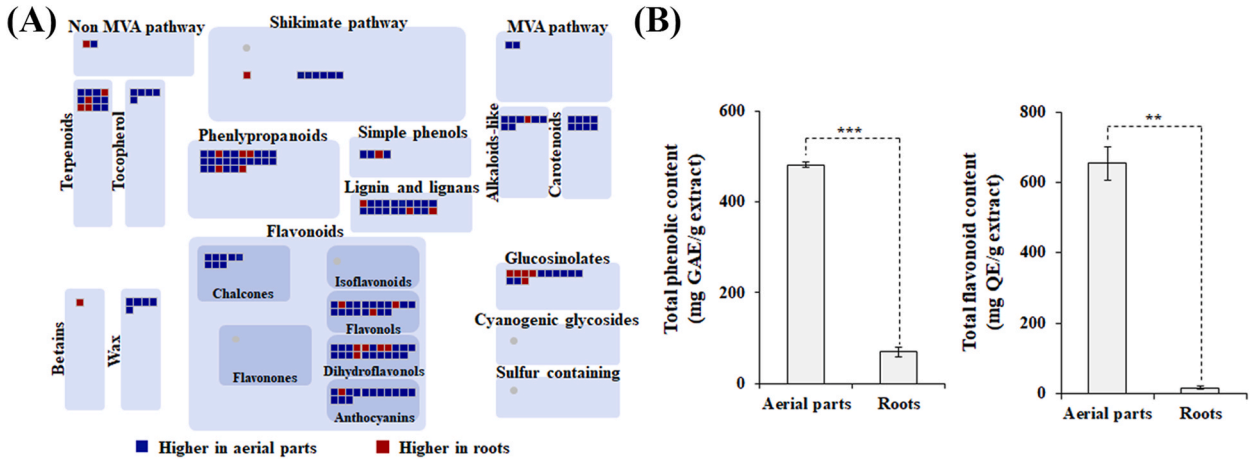

Fig. 4. Classification of DEGs based on (A) Mapman secondary metabolism category and (B) the variations in total phenolic (TPC) and total flavonoid (TFC) contents between the aerial parts and roots. Data represent the mean (±SE) of three independent experiments. Significance: $^{**}p < 0.01$ and $^{***}p < 0.005$ (*t*-test).

shown in Fig. 5A, the two putative AbtYABBYs exhibited a distinct structural arrangement, featuring a C2C2 type zinc finger domain at the N-terminus and a YABBY domain at the C-terminus. Additionally, AdtYABBY1 and AdtYABBY2 were clustered in the YAB5 clade together with AaYABBY5 (Supplementary Fig. 3), suggesting that they belong to the YABBY family. To investigate the function of AdtYABBY1 and AdtYABBY2, *Agrobacterium* cells carrying the overexpression constructs of the corresponding genes were infiltrated into tobacco leaves. As shown in Fig. 5B, the transient expression of AdtYABBY1 and AdtYABBY2 led to a 1.69- and 1.53-fold increase in flavonoid production, respectively, compared to leaves overexpressing GUS (Mock control). Additionally, the expression of phenylpropanoid biosynthetic genes was significantly induced by AdtYABBY1 and AdtYABBY2 (Fig. 5C). Furthermore, the presence of light-responsive elements in plant YABBY promoters suggests that YABBYs are regulated by light [55,56]. These results indicate that AdtYABBY1 and AdtYABBY2 act as positive regulators of phenylpropanoid biosynthesis, implying that these YABBY proteins likely stimulate the light-dependent production of polyphenolic compounds in aerial parts.

4. Conclusion

In conclusion, the present study sheds light on the intricate spatial dynamics of secondary metabolites in *A. triphylla*, underscoring the importance of tissue-specific metabolic profiling in understanding plant bioactivity. The anti-inflammatory properties of A_EtF exhibited an IC_{50} value of 27.2 ± 2.3 μg/mL, significantly superior to that of R_EtF with an IC_{50} of 38.9 ± 2.9 μg/mL. Similarly, the anti-melanogenic activity of A_EtF (IC_{50} = 68.9 ± 2.3 μg/mL) surpassed that of R_EtF (IC_{50} = 90.0 ± 5.5 μg/mL), indicating that the aerial parts and roots of A. triphylla exhibit distinct bioactive properties. Metabolome and transcriptome analyses indicated the crucial role of spatially regulated genes in mediating secondary metabolite accumulation. Furthermore, transient expression of the TFs AdtYABBY1 and AdtYABBY2 in tobacco leaves resulted in enhanced flavonoid production, indicating their positive regulatory role in polyphenolic compound biosynthesis. By elucidating the complex interplay between spatial metabolism and pharmacological activity, the present study lays the groundwork for the development of novel herbal remedies and pharmaceuticals derived from *A. triphylla*. Detailed investigations into the signal transduction pathways and gene networks involved in the tissue-specific accumulation of secondary metabolites could provide deeper insights into their regulation. Additionally, exploring the environmental factors that influence key transcription factors like AdtYABBY1 and AdtYABBY2 could pave the way for the targeted enhancement of bioactive compound production. Further research elucidating the regulatory mechanisms governing spatial metabolite distribution will also aid in the precise manipulation of plant bioactivity for therapeutic and industrial applications.

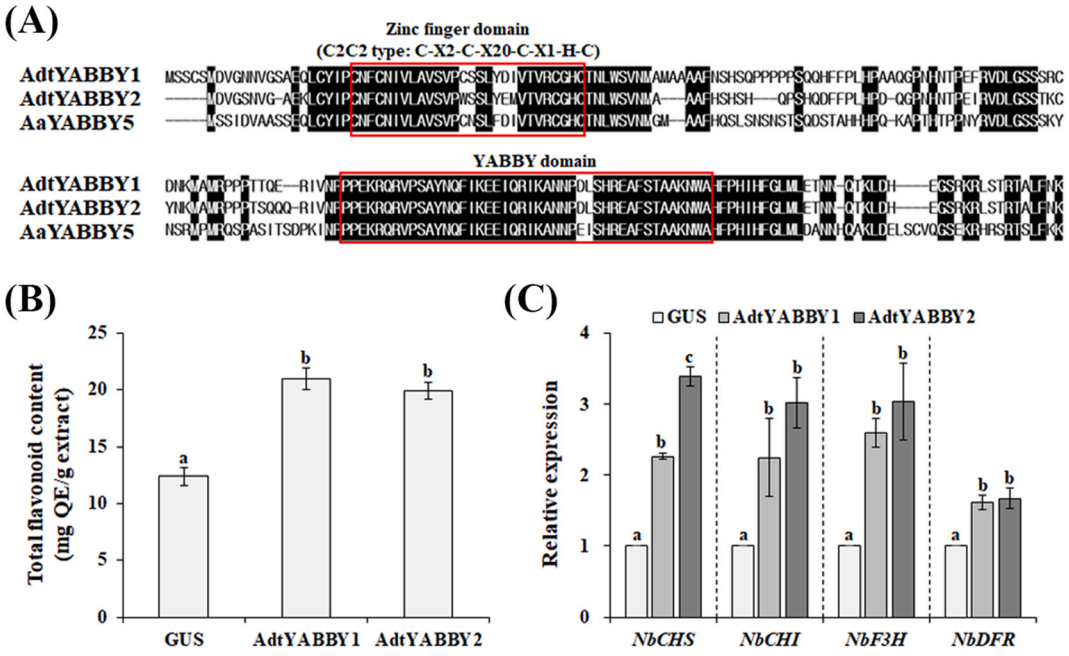

Fig. 5. Functional characterization of AdtYABBY1 and AdtYABBY2. (A) Multiple sequence alignment of AdtYABBY1 and AdtYABBY2 with AaYABBY5. (B) TFC and (C) the expression of phenylpropanoid biosynthetic genes in tobacco leaves transiently expressing AdtYABBY1 or AdtYABBY2. The transcription level of each gene in every sample was normalized to the mock control (GUS-expressing leaves). Data represent the mean (±SE) of three independent experiments, with distinct letters ($p < 0.05$, Duncan's multiple range test) indicating statistically significant differences. NbCHS, *N*icotiana *benthamiana* chalcone synthase; NbCHI, *N. benthamiana* chalcone isomerase; NbF3H, *N. benthamiana* flavanone 3-hydroxylase; NbDFR, *N. benthamiana* dihydroflavonol reductase.

Data availability statement

Data will be made available on request.

CRediT authorship contribution statement

Seon Young Yoon: Writing – original draft, Investigation, Data curation. **Seon-Woong Kim:** Formal analysis, Data curation. **Tae Kyung Hyun:** Writing – review & editing, Writing – original draft, Visualization, Conceptualization.

Declaration of competing interest

The authors declare the following financial interests/personal relationships which may be considered as potential competing interests:Tae Kyung Hyun reports financial support was provided by Regional Innovation Strategy (RIS). If there are other authors, they declare that they have no known competing financial interests or personal relationships that could have appeared to influence the work reported in this paper.

Acknowledgement

This research was supported by "Regional Innovation Strategy (RIS)" through the National Research Foundation of Korea (NRF) funded by the Ministry of Education (MOE) (2021RIS-001, 1345370811).

Appendix A. Supplementary data

Supplementary data to this article can be found online at https://doi.org/10.1016/j.heliyon.2024.e37898.

References

[1] L. Yang, K.S. Wen, X. Ruan, Y.X. Zhao, F. Wei, Q. Wang, Response of plant secondary metabolites to environmental factors, Molecules 23 (2018) 762, https://doi.org/10.3390/molecules23040762.
[2] D.M. Pott, S. Osorio, J.G. Vallarino, From central to specialized metabolism: an overview of some secondary compounds derived from the primary metabolism for their role in conferring nutritional and organoleptic characteristics to fruit, Front. Plant Sci. 10 (2019) 835, https://doi.org/10.3389/fpls.2019.00835.
[3] A. Rai, M. Yamazaki, H. Takahashi, M. Nakamura, M. Kojoma, H. Suzuki, K. Saito, RNA-seq transcriptome analysis of *Panax japonicus*, and its comparison with other panax species to identify potential genes involved in the saponins biosynthesis, Front. Plant Sci. 7 (2016) 481, https://doi.org/10.3389/fpls.2016.00481.
[4] T. Hashimoto, Y. Yamada, New genes in alkaloid metabolism and transport, Curr. Opin. Biotechnol. 14 (2003) 163–168, https://doi.org/10.1016/s0958-1669(03)00027-2.
[5] C.Q. Yang, X. Fang, X.M. Wu, Y.B. Mao, L.J. Wang, X.Y. Chen, Transcriptional regulation of plant secondary metabolism, J. Integr. Plant Biol. 54 (2012) 703–712, https://doi.org/10.1111/j.1744-7909.2012.01161.x.
[6] N. Shitan, Secondary metabolites in plants: transport and self-tolerance mechanisms, Biosci. Biotechnol. Biochem. 80 (2016) 1283–1293, https://doi.org/10.1080/09168451.2016.1151344.
[7] M. Ekor, The growing use of herbal medicines: issues relating to adverse reactions and challenges in monitoring safety, Front. Pharmacol. 4 (2014) 177, https://doi.org/10.3389/fphar.2013.00177.
[8] S. Bafandeh, E. Khodadadi, K. Ganbarov, M. Asgharzadeh, Ş. Köse, H. Samadi Kafil, Natural products as a potential source of promising therapeutics for COVID-19 and viral diseases, Evid. Based Complement Alternat, Med. 2023 (2023) 5525165, https://doi.org/10.1155/2023/5525165.
[9] L.H. Miller, X. Su, Artemisinin: discovery from the Chinese herbal garden, Cell 146 (2011) 855–858, https://doi.org/10.1016/j.cell.2011.08.024.
[10] H. Dong, J. Ma, T. Li, Y. Xiao, N. Zheng, J. Liu, Y. Gao, J. Shao, L. Jia, Global deregulation of ginseng products may be a safety hazard to warfarin takers: solid evidence of ginseng-warfarin interaction, Sci. Rep. 7 (2017) 5813, https://doi.org/10.1038/s41598-017-05825-9.
[11] H. Wang, D. Peng, J. Xie, Ginseng leaf-stem: bioactive constituents and pharmacological functions, Chin. Med. 4 (2009) 20, https://doi.org/10.1186/1749-8546-4-20.
[12] T.K. Hyun, K.I. Jang, Are berries useless by-products of ginseng? Recent research on the potential health benefits of ginseng berry, EXCLI J 16 (2017) 780–784, https://doi.org/10.17179/excli2017-376.
[13] Y.C. Zhang, G. Li, C. Jiang, B. Yang, H.J. Yang, H.Y. Xu, L.Q. Huang, Tissue-specific distribution of ginsenosides in different aged ginseng and antioxidant activity of ginseng leaf, Molecules 19 (2014) 17381–17399, https://doi.org/10.3390/molecules191117381.
[14] J. Kim, S.Y. Cho, S.H. Kim, D. Cho, S. Kim, C.W. Park, T. Shimizu, J.Y. Cho, D.B. Seo, S.S. Shin, Effects of Korean ginseng berry on skin antipigmentation and antiaging via FoxO3a activation, J. Ginseng Res. 41 (2017) 277–283, https://doi.org/10.1016/j.jgr.2016.05.005.
[15] S. Jin, S.H. Eom, J.-S. Kim, I.H. Jo, T.K. Hyun, Influence of ripening stages on phytochemical composition and bioavailability of ginseng berry (*Panax ginseng* C. A. Meyer), J. Appl. Bot. Food Qual. 92 (2019) 130–137, https://doi.org/10.5073/JABFQ.2019.092.018.
[16] F. Zhang, S. Tang, L. Zhao, X. Yang, Y. Yao, Z. Hou, P. Xue, Stem-leaves of Panax as a rich and sustainable source of less-polar ginsenosides: comparison of ginsenosides from *Panax ginseng*, American ginseng and *Panax notoginseng* prepared by heating and acid treatment, J. Ginseng Res. 45 (2021) 163–175, https://doi.org/10.1016/j.jgr.2020.01.003.
[17] S.H. Park, Ethyl acetate fraction of *Adenophora triphylla* var. japonica inhibits migration of lewis lung carcinoma cells by suppressing macrophage polarization toward an M2 phenotype, J. Pharmacopuncture 22 (2019) 253–259, https://doi.org/10.3831/KPI.2019.22.034.
[18] S.Y. Yoo, S.K. Park, J.Y. Kang, J.M. Kim, S.H. Park, B.S. Kwon, C.J. Lee, J.E. Kang, S.B. Park, U. Lee, H.J. Hea, Skin whitening effect of ethyl acetate fraction of *Adenophora triphylla* var. japonica Sprout, Korean J. Polar Res. 30 (2017) 352–363, https://doi.org/10.7732/kjpr.2017.30.4.352.
[19] J. Chun, M. Kang, Y.S. Kim, A triterpenoid saponin from *Adenophora triphylla* var. japonica suppresses the growth of human gastric cancer cells via regulation of apoptosis and autophagy, Tumour Biol 35 (2014) 12021–12030, https://doi.org/10.1007/s13277-014-2501-0.
[20] D.R. Lee, Y.S. Lee, B.K. Choi, H.J. Lee, S.B. Park, T.M. Kim, H.J. Oh, S.H. Yang, J.W. Suh, Roots extracts of *Adenophora triphylla* var. japonica improve obesity in 3T3-L1 adipocytes and high-fat diet-induced obese mice, Asian Pac. J. Tropical Med. 8 (2015) 898–906, https://doi.org/10.1016/j.apjtm.2015.10.011.

[21] J.-R. Hu, C.-J. Jung, S.-M. Ku, D.-H. Jung, S.-K. Ku, J.-S. Choi, Antitussive, expectorant, and anti-inflammatory effects of Adenophorae Radix powder in ICR mice, J. Ethnopharmacol. 239 (2019) 111915, https://doi.org/10.1016/j.jep.2019.111915.
[22] H.L. Kim, H.J. Lee, B.-K. Choi, S.-B. Park, S.M. Woo, D.-R. Lee, Roots extract of *Adenophora triphylla* var. japonica inhibits adipogenesis in 3T3-L1 cells through the downregulation of IRS1, J. Physiol. Pathol. Korean Med. 34 (2020) 136–141, https://doi.org/10.15188/kjopp.2020.06.34.3.136.
[23] H.J. Park, S.H. Park, Hexane fraction of *Adenophora triphylla* var. japonica root extract induces apoptosis of human lung cancer cells by inactivating Src/STAT3 pathway, Nat. Prod. Res. 28 (2022) 1–5, https://doi.org/10.1080/14786419.2022.2137503.
[24] K. Hori, H.P. Devkota, Phenolic Compounds from the aerial parts of *Adenophora triphylla* (Thunb.) A. DC. var. triphylla and their free radical scavenging activity, Nepal, J. Biotechnol. 8 (2020) 12–16, https://doi.org/10.3126/njb.v8i1.30205.
[25] G. Kim, T.K. Hyun, Influence of flower bud removal on the growth and anti-inflammatory properties of *Platycodon grandiflorus* roots, Ind. Crop. Prod. 195 (2023) 116389, https://doi.org/10.1016/j.indcrop.2023.116389.
[26] M.-A. Ahn, J. Lee, T.K. Hyun, Histone deacetylase inhibitor, sodium butyrate-induced metabolic modulation in *Platycodon grandiflorus* roots enhances anti-melanogenic properties, Int. J. Mol. Sci. 24 (2023) 11804, https://doi.org/10.3390/ijms241411804.
[27] S.G. Bang, M.-A. Ahn, S.H. Eom, W.T. Joeng, T.K. Hyun, Methyl jasmonate enhances the anti-inflammatory effects of the adventitious roots in *Abeliophyllum distichum* by increasing the production of polyphenolic compounds, Rev. Mex. Ing. Quim. 21 (2022) Bio2819, https://doi.org/10.24275/rmiq/Bio2819.
[28] D.-U. Shin, J.-E. Eom, H.-J. Song, S.Y. Jung, T.V. Nguyen, K.M. Lim, O.H. Chai, H.-J. Kim, G.-D. Kim, H.S. Shin, S.-Y. Lee, *Camellia sinensis* L. alleviates pulmonary inflammation induced by porcine pancreas elastase and cigarette smoke extract, Antioxidants 11 (2022) 1683, https://doi.org/10.3390/antiox11091683.
[29] J.H. Choi, H. Kim, T.K. Hyun, Transcriptome analysis of *Abeliophyllum distichum* NAKAI reveals potential molecular markers and candidate genes involved in anthocyanin biosynthesis pathway, S. Afr. J. Bot. 116 (2018) 34–41, https://doi.org/10.1016/j.sajb.2018.02.401.
[30] B.J. Haas, A. Papanicolaou, M. Yassour, M. Grabherr, P.D. Blood, J. Bowden, M.B. Couger, D. Eccles, B. Li, M. Lieber, M.D. MacManes, M. Ott, J. Orvis, N. Pochet, F. Strozzi, N. Weeks, R. Westerman, T. William, C.N. Dewey, R. Henschel, R.D. LeDuc, N. Friedman, A. Regev, De novo transcript sequence reconstruction from RNA-seq using the Trinity platform for reference generation and analysis, Nat. Protoc. 8 (2013) 1494–1512, https://doi.org/10.1038/nprot.2013.084.
[31] E. Kim, T.K. Hyun, PlgMYBR1, an R2R3-MYB transcription factor, plays as a negative regulator of anthocyanin biosynthesis in *Platycodon grandiflorus*, 3 Biotech 13 (2023) 75, https://doi.org/10.1007/s13205-023-03490-6.
[32] S. Khatua, J. Simal-Gandara, K. Acharya, Understanding immune-modulatory efficacy in vitro, Chem. Biol. Interact. 352 (2022) 109776, https://doi.org/10.1016/j.cbi.2021.109776.
[33] J.H. Kim, J.Y. Hong, S.R. Shin, K.Y. Yoon, Comparison of antioxidant activity in wild plant (*Adenophora triphylla*) leaves and roots as a potential source of functional foods, Int. J. Food Sci. Nutr. 60 (2009) 150–161, https://doi.org/10.1080/09637480902956594.
[34] Y.X. Han, P.F. Wang, M. Zhao, L.M. Chen, Z.M. Wang, X.Q. Liu, H.M. Gao, M.X. Gong, H. Li, J.Z. Zhu, C.G. Liu, Chemical profiling of xueshuan xinmaining tablet by HPLC and UPLC-ESI-Q-TOF/MS, Evid. Based Complement. Altern. Med. 2018 (2018) 2781597, https://doi.org/10.1155/2018/2781597.
[35] S.J. Wi, S.Y. Seo, K. Cho, M.H. Nam, K.Y. Park, Lysophosphatidylcholine enhances susceptibility in signaling pathway against pathogen infection through biphasic production of reactive oxygen species and ethylene in tobacco plants, Phytochemistry 104 (2014) 48–59, https://doi.org/10.1016/j.phytochem.2014.04.009.
[36] B. Gullón, T.A. Lú-Chau, M.T. Moreira, J.M. Lema, G. Eibes, Rutin: a review on extraction, identification and purification methods, biological activities and approaches to enhance its bioavailability, Trends Food Sci. Technol. 67 (2017) 220–235, https://doi.org/10.1016/j.tifs.2017.07.008.
[37] G. Shabir, A. Saeed, H.R. El-Seedi, Natural isocoumarins: structural styles and biological activities, the revelations carry on, Phytochemistry 181 (2021) 112568, https://doi.org/10.1016/j.phytochem.2020.112568.
[38] Y. Zheng, R. Zhang, W. Shi, L. Li, H. Liu, Z. Chen, L. Wu, Metabolism and pharmacological activities of the natural health-benefiting compound diosmin, Food Funct. 11 (2020) 8472–8492, https://doi.org/10.1039/d0fo01598a.
[39] B. Kuai, J. Chen, S. Hörtensteiner, The biochemistry and molecular biology of chlorophyll breakdown, J. Exp. Bot. 69 (2018) 751–767, https://doi.org/10.1093/jxb/erx322.
[40] A. Saide, C. Lauritano, A. Ianora, Pheophorbide a: state of the art, Mar. Drugs 18 (2020) 257, https://doi.org/10.3390/md18050257.
[41] H. Lee, H.Y. Park, T.S. Jeong, Pheophorbide a derivatives exert antiwrinkle effects on UVB-induced skin aging in human fibroblasts, Life 11 (2021) 147, https://doi.org/10.3390/life11020147.
[42] H. Lefevere, L. Bauters, G. Gheysen, Salicylic acid biosynthesis in plants, Front. Plant Sci. 11 (2020) 338, https://doi.org/10.3389/fpls.2020.00338.
[43] M. Yang, A. Ismayil, Z. Jiang, Y. Wang, X. Zheng, L. Yan, Y. Hong, D. Li, Y. Liu, A viral protein disrupts vacuolar acidification to facilitate virus infection in plants, EMBO J. 41 (2022) e108713, https://doi.org/10.15252/embj.2021108713.
[44] H.F. Liu, X.J. Xue, Y. Yu, M.M. Xu, C.C. Lu, X.L. Meng, B.G. Zhang, X.H. Ding, Z.H. Chu, Copper ions suppress abscisic acid biosynthesis to enhance defence against Phytophthora infestans in potato, Mol. Plant Pathol. 21 (2020) 636–651, https://doi.org/10.1111/mpp.12919.
[45] Y. Yuan, J. Zhang, X. Liu, M. Meng, J. Wang, J. Lin, Tissue-specific transcriptome for *Dendrobium officinale* reveals genes involved in flavonoid biosynthesis, Genomics 112 (2020) 1781–1794, https://doi.org/10.1016/j.ygeno.2019.10.010.
[46] D.J. Yin, S.J. Ye, X.Y. Sun, Q.Y. Chen, T. Min, H.X. Wang, L.M. Wang, Integrative analysis of the transcriptome and metabolome reveals genes involved in phenylpropanoid and flavonoid biosynthesis in the *Trapa bispinosa* Roxb, Front. Plant Sci. 13 (2022) 913265, https://doi.org/10.3389/fpls.2022.913265.
[47] Y. Zhou, X. Xu, Y. Chen, J. Gao, Q. Shi, L. Tian, L. Cao, Combined metabolome and transcriptome analyses reveal the flavonoids changes and biosynthesis mechanisms in different organs of *Hibiseu manihot* L, Front. Plant Sci. 13 (2022) 817378, https://doi.org/10.3389/fpls.2022.817378.
[48] R. Zhou, W.H. Su, G.F. Zhang, Y.N. Zhang, X.R. Guo, Relationship between flavonoids and photoprotection in shade-developed Erigeron breviscapus transferred to sunlight, Photosynthetica 54 (2016) 201–209, https://doi.org/10.1007/s11099-016-0074-4.
[49] Y. Liu, S. Fang, W. Yang, X. Shang, X. Fu, Light quality affects flavonoid production and related gene expression in *Cyclocarya paliurus*, J. Photochem. Photobiol. B Biol. 179 (2018) 66–73, https://doi.org/10.1016/j.jphotobiol.2018.01.002.
[50] Y.W. Ni, K.H. Lin, K.H. Chen, C.W. Wu, Y.S. Chang, Flavonoid compounds and photosynthesis in passiflora plant leaves under varying light intensities, Plants 9 (2020) 633, https://doi.org/10.3390/plants9050633.
[51] J. Naik, P. Misra, P.K. Trivedi, A. Pandey, Molecular components associated with the regulation of flavonoid biosynthesis, Plant. Sci. 317 (2022) 111196, https://doi.org/10.1016/j.plantsci.2022.111196.
[52] M. Boter, J.F. Golz, S. Giménez-Ibañez, G. Fernandez-Barbero, J.M. Franco-Zorrilla, R. Solano, FILAMENTOUS FLOWER Is a direct target of JAZ3 and modulates responses to jasmonate, Plant Cell 27 (2015) 3160–3174, https://doi.org/10.1105/tpc.15.00220.
[53] S.I. Kayani, Q. Shen, S.U. Rahman, X. Fu, Y. Li, C. Wang, D. Hassani, K. Tang, Transcriptional regulation of flavonoid biosynthesis in *Artemisia annua* by AaYABBY5, Hortic. Res. 8 (2021) 257, https://doi.org/10.1038/s41438-021-00693-x.
[54] S. Zhao, Y. Zhang, M. Tan, J. Jiao, C. Zhang, P. Wu, K. Feng, L. Li, Identification of YABBY transcription factors and their function in ABA and salinity response in *Nelumbo nucifera*, Plants 12 (2023) 380, https://doi.org/10.3390/plants12020380.
[55] S. Yin, S. Li, Y. Gao, E.S. Bartholomew, R. Wang, H. Yang, C. Liu, X. Chen, Y. Wang, X. Liu, H. Ren, Genome-wide identification of YABBY gene family in Cucurbitaceae and expression analysis in cucumber (*Cucumis sativus* L.), Genes 13 (2022) 467, https://doi.org/10.3390/genes13030467.
[56] L. Kong, J. Sun, Z. Jiang, W. Ren, Z. Wang, M. Zhang, X. Liu, L. Wang, W. Ma, J. Xu, Identification and expression analysis of YABBY family genes in *Platycodon grandiflorus*, Plant Signal. Behav. 18 (2023) 2163069, https://doi.org/10.1080/15592324.2022.2163069.